IOP Conf. Series: Journal of Physics: Conf. Series **1023** (2018) 012023 doi:10.1088/1742-6596/1023/1/012023

Signatures of triaxiality in low-spin spectra of ^{86}Ge

M. Lettmann[1], V. Werner[1], N. Pietralla[1], P. Doornenbal[2], A. Obertelli[3,2,1], T.R. Rodríguez[4], K. Sieja[5], G. Authelet[3], H. Baba[2], D. Calvet[3], F. Château[3], S. Chen[2,6], A. Corsi[3], A. Delbart[3], J.-M. Gheller[3], A. Giganon[3], A. Gillibert[3], V. Lapoux[3], T. Motobayashi[2], M. Niikura[7], N. Paul[2,3], J.-Y. Roussé[3], H. Sakurai[2,7], C. Santamaria[3], D. Steppenbeck[2], R. Taniuchi[2,7], T. Uesaka[2], T. Ando[2,7], T. Arici[8], A. Blazhev[9], F. Browne[10], A. Bruce[10], R.J. Caroll[11], L.X. Chung[12], M.L. Cortés[1,2,8], M. Dewald[9], B. Ding[13], F. Flavigny[14], S. Franchoo[14], M. Górska[8], A. Gottardo[14], A. Jungclaus[15], J. Lee[16], B.D. Linh[12], J. Liu[16], Z. Liu[13], C. Lizarazo[1,8], S. Momiyama[2,7], K. Moschner[9], S. Nagamine[7], N. Nakatsuka[17], C. Nita[18], C.R. Nobs[10], L. Olivier[14], Z. Patel[11], Zs. Podolyák[11], M. Rudigier[11], T. Saito[7], C. Shand[11], P.-A. Söderström[1,2,8], I. Stefan[14], V. Vaquero[15], K. Wimmer[7], Z. Xu[16,19]

[1] Institut für Kernphysik, Technische Universität Darmstadt, 64289 Darmstadt, Germany
[2] RIKEN Nishina Center, 2-1 Hirosawa, Wako, Saitama 351-0198, Japan
[3] CEA, Centre de Saclay, IRFU/Service de Physique Nucléaire, 91191 Gif-sur-Yvette, France
[4] Departamento de Física Teórica, Universidad Autónoma de Madrid, 28049, Spain
[5] IPHC, CNRS/IN2P3 et Université de Strasbourg, 67037 Strasbourg, France
[6] State Key Laboratory of Nuclear Physics and Technology, Peking University, Beijing 100871, P.R. China
[7] Department of Physics, University of Tokyo, 7-3-1 Hongo, Bunkyo, Tokyo 113-0033, Japan
[8] GSI Helmholtzzentrum für Schwerionenforschung GmbH, 64291 Darmstadt, Germany
[9] Institut für Kernphysik, Universität zu Köln, 50937 Köln, Germany
[10] School of Computing Engineering and Mathematics, University of Brighton, Brighton BN2 4GJ, United Kingdom
[11] Department of Physics, University of Surrey, Guildford GU2 7XH, United Kingdom
[12] Institute for Nuclear Science & Technology, VINATOM, P.O. Box 5T-160, Nghia Do, Hanoi, Vietnam
[13] Institute of Modern Physics, Chinese Academy of Sciences, Lanzhou 730000, P.R. China
[14] Institut de Physique Nucléaire Orsay, IN2P3-CNRS, 91406 Orsay Cedex, France
[15] Instituto de Estructura de la Materia, CSIC, 28006 Madrid, Spain
[16] Department of Physics, The University of Hong Kong, Pokfulam, Hong Kong
[17] Department of Physics, Faculty of Science, Kyoto University, Kyoto 606-8502, Japan
[18] Horia Hulubei National Institute of Physics and Nuclear Engineering (IFIN-HH), 077125 Bucharest, Romania
[19] KU Leuven, Instituut voor Kern- en Stralingsfysica, 3001 Leuven, Belgium

E-mail: mlettmann@ikp.tu-darmstadt.de

Abstract. Low-spin states of neutron-rich ^{84,86,88}Ge were measured by in-flight γ-ray spectroscopy at 270 MeV/u at the RIKEN-RIBF facility. The exotic beams have been produced by primary ^{238}U in-flight fission reactions and impinged on the MINOS device. MINOS combines a 10-cm long LH_2 target with a Time Projection Chamber (TPC) to reconstruct the reaction vertices. The reactions were selected by the BigRIPS and the ZeroDegree spectrometers for

the incoming and outgoing channels, respectively. Emitted γ radiation was detected by the NaI-array DALI2. De-excitations from the 6_1^+, $4_{1,2}^+$, and $2_{1,2}^+$ states of ^{84,86}Ge and 4_1^+ and $2_{1,2}^+$ states of ^{88}Ge were observed. The data are compared to state-of-the-art shell model and beyond-mean-field calculations. Furthermore, a candidate for a 3_1^+ state of ^{86}Ge was identified. This state plays a key role in the discussion of ground-state triaxiality of ^{86}Ge, along with other features of the low-energy level scheme. This work was published in [1].

1. Introduction

For many years triaxial nuclei have been of high interest in nuclear structure physics. More than 60 years ago two elementary models, introducing a breaking of the axial symmetry of the Bohr Hamiltonian [2], were derived. In these models the deformation is described by the triaxial deformation parameter γ, ranging from 0° (prolate shape) to 60° (oblate shape), and the axial elongation β. A deformation parameter $\gamma = 30°$ reflects the maximum of triaxiality. On one hand, the model by Wilets and Jean [3] assumes a potential energy surface independent of γ, which is referred to as the γ-soft case. On the other hand the rigid triaxial rotor model, by Davydov and Filippov [4], describes the potential energy surface with a distinct minimum for a certain value of γ.

The low-spin spectra of a rigid triaxial rotor and a γ-soft nucleus show strong similarities. Of particular importance is the (quasi-)γ-band head positioned at low energy, typically below the yrast-4^+ state. This unique feature clearly differentiates them from axially symmetric rotors, which show high energies of the γ band. In order to distinguish between the spectra of a rigid triaxial rotor and a γ-soft nucleus the energy difference of the odd and even members is a key part, especially the difference between the 3_γ^+ and 2_γ^+ states compared to the difference of the 3_γ^+ and 4_γ^+ states. While in case of a rigid triaxial rotor the odd-spin states are closer to the lower-lying even-spin states, in a γ-soft nucleus they are closer to the higher-lying states. This fact is usually referred to as staggering $S(J)$ [5, 6] and is described by

$$S(J) = \frac{[E(J) - E(J-1)] - [E(J-1) - E(J-2)]}{E(2_1^+)}, \tag{1}$$

with the spin J. For a rigid triaxial rotor the $S(4)$ is positive. So far only ^{76}Ge [7] has an experimentally-derived positive $S(4)$ value and shows a significant degree of rigid triaxiality in the medium mass region $A < 100$.

2. Experimental setup

The experiment was conducted at the Radioactive Isotope Beam Factory (RIBF). A ^{238}U beam was accelerated to an energy of 345 MeV/u and impinged on a 3-mm-thick ^{9}Be production target at the entrance of the BigRIPS fragment separator [8]. This lead to a cocktail of different nuclei produced by in flight-fission. The isotopes of interest were selected by the $B\rho$-ΔE-$B\rho$ method in the BigRIPS fragment separator, while the particle identification was performed on an event-by-event basis by the time of flight-$B\rho$-ΔE method [9]. ^{87}As and ^{85}Ge were produced in one setting with a measurement time of $\sim$ 22 h, with rates of 2059 and 731 s^{-1}, respectively. An additional setting was utilized to provide ^{89}As with rates of 140 s^{-1} for $\sim$ 10.5 h. At the end of the BigRIPS fragment separator, the selected nuclei impinged on the 99(1)-mm-thick liquid-hydrogen reaction target of MINOS [10] with an kinetic energy of $\sim$ 270 MeV/u. While passing the target cell the ion's kinetic energy was reduced by $\sim$ 70 MeV/u. In the following, we focus on (p, pn) and $(p, 2p)$ reaction channels. The resulting reaction products were identified by the $B\rho$-ΔE-$B\rho$ method in the ZeroDegree spectrometer [8]. The reaction vertices of the protons

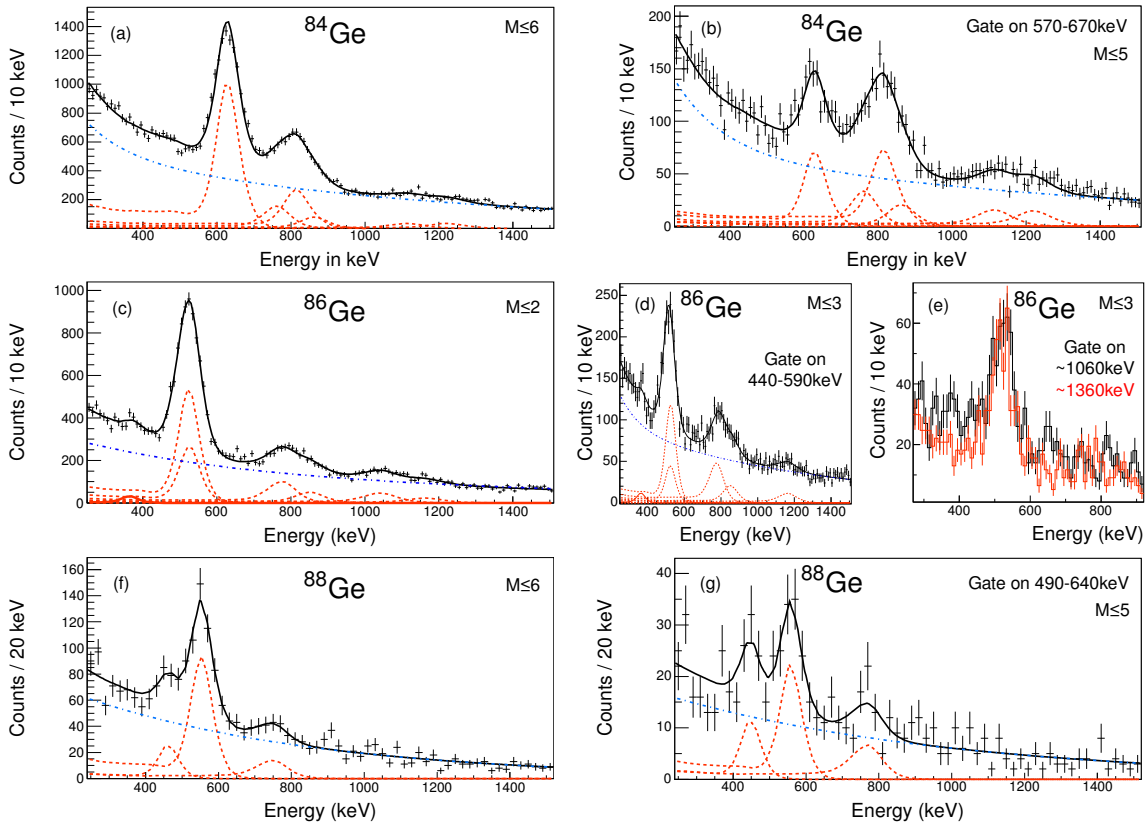

Figure 1. Doppler-corrected DALI2 spectra obtained in the reactions (a) ^{85}Ge(p,pn)^{84}Ge, (c) ^{87}As(p,2p)^{86}Ge, (f) ^{89}As(p,2p)^{88}Ge are shown as black data points, superimposed with the fit of the whole spectrum (black solid line). The respective background (blue dash dotted line) and simulated response functions for each transition (red dotted and solid lines) are shown. Spectra (b), (d), (g) show gates on the 2_1^+ regions. In (e) also gates on the $2_2^+ \rightarrow 0_1^+$ (black), and a neighboring region (red) are shown. The multiplicity cutoff M for ^{86}Ge is chosen to optimize the background-to-peak ratio according to available statistics. For ^{84}Ge higher M is chosen to enhance higher-lying transitions and for ^{88}Ge because of the low statistics. An addback distance of 15 cm was applied to produce the shown spectra.

emitted during (p, pn) or $(p, 2p)$ reactions were reconstructed by the time projection chamber (TPC) of MINOS, which was surrounding the liquid-hydrogen target. The vertex resolution of MINOS is $\lesssim$ 5 mm $FWHM$ and the possibility to detect at least one proton from a $(p, 2p)$ channel is $\gtrsim$ 92% . The de-excitation γ rays were detected by the NaI(Tl) scintillator array DALI2 [12], covering polar angles from 0° to 128° with respect to the center of MINOS. The combination of MINOS and DALI2 was successfully used in the past [13, 14, 15, 16, 17, 18, 19]. A full-energy peak detection efficiency of 35% (23%) was obtained for a 500-keV (1-MeV) γ ray by a simulation within the GEANT4 framework [20] for the DALI2 array. For that, the emission of a γ ray from a nucleus in the center of the MINOS target moving with a kinetic energy of 250 keV, was simulated. Five transitions between 662 keV and 1836 keV of ^{137}Cs, ^{88}Y and ^{60}Co sources were used for the energy calibrations. A calibration error of 1.5 keV was estimated for the energy calibration, while an energy resolution of 9% (6%) FWHM at 662 keV (1.332 MeV) was determined.

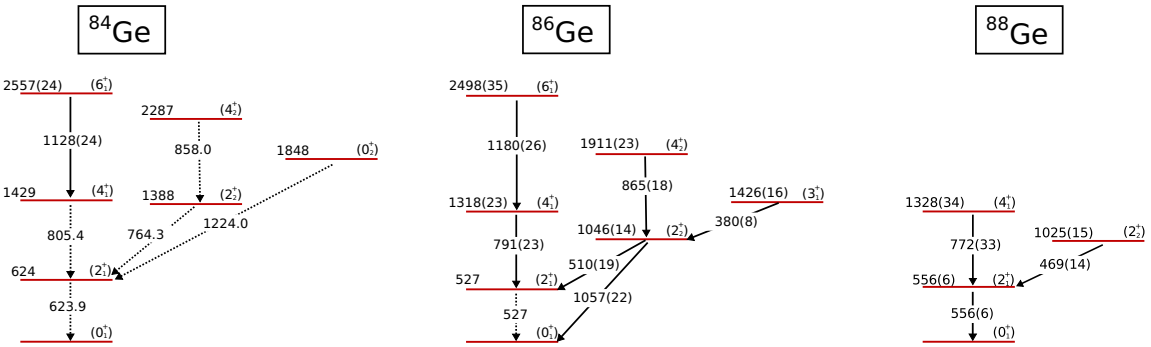

Figure 2. Measured transition energies and proposed level energies of ^{84,86,88}Ge. Dashed arrows denote transition energies taken from literature [21, 22, 23, 24] and solid arrows mark transitions measured for the first time. The tentative spin assignments for ^{84}Ge are taken from [21] (see text).

3. Results

Figure 1 shows the Doppler-corrected γ-ray spectra obtained after the reactions ^{85}Ge(p,pn)^{84}Ge, ^{87}As(p,2p)^{86}Ge, ^{89}As(p,2p)^{88}Ge. The experimental spectra are described by a least-square fit of the DALI2 response function of the γ-ray transitions combined with a two-component experimental background. The DALI2 response function is derived by a Monte Carlo simulation. The uncertainties of the measured transition energies consist of three contributions: a statistical uncertainty due to the fitting procedure, an uncertainty from the energy calibration, and an uncertainty caused by lifetime dependent Doppler broadening and shifts of the observed transitions. An upper limit for the lifetimes is obtained by a χ^2 analysis and is in agreement with theory predictions (see below).

The Doppler-corrected γ spectrum from the reaction ^{85}Ge(p,pn)^{84}Ge is shown in figure 1 (a). Since many γ-ray transition energies are known from β-delayed spectroscopy [21, 22, 23] the reaction serves as a test case. In total six transitions are observed at energies of 629(7) keV, 772(18) keV, 813(10) keV, 867(13) keV, 1128(24) keV and 1229(15) keV. The transition at 1128(24) keV is observed for the first time. The observations are in good agreement with [21] and the proposed level scheme is shown in figure 2 on the left. Since the presented experiment is not sensitive to the spins of the observed states they are tentatively assigned. However, based on systematics of neighboring Ge isotopes the 1128(24)-keV transition is assigned to the $(6_1^+) \rightarrow 4_1^+$ transition. A $\gamma\gamma$-coincidence gate on the energy range of the $2_1^+ \rightarrow 0_1^+$ transition energy is shown in figure 1 (b). Note, that the 629(7)-keV transition still appears in the coincidence condition, due to coincidences with Compton events of higher-energy transitions underneath the 629(7)-keV lineshape, though strongly reduced. ^{86}Ge is produced by a ^{87}As(p,2p) reaction, and the Doppler-corrected spectrum is shown in figure 1 (c). Seven transitions at energies of 380(8) keV, 510(19) keV, 534(8) keV, 791(23) keV, 865(18) keV, 1057(22) keV and 1180(26) keV are identified. The transition at 534(8) keV was observed before via β-decay studies [24] and is in good agreement with the results of this work. The assignment to the decay of the $2_1^+ \rightarrow 0_1^+$ is adopted. The proposed level scheme for ^{86}Ge is shown in the middle of figure 2, based on the following argumentation. The strongest observed γ decay in the spectrum stems from the $2_1^+ \rightarrow 0_1^+$ transition for an even-even nucleus populated via $(p, 2p)$ (see, e.g., [25, 26, 27, 28]). Furthermore, the second strongest transition corresponds to the $(4_1^+) \rightarrow (2_1^+)$ transition. Figure 1 (d) shows a $\gamma\gamma$ coincidence condition on the energy range of the $2_1^+ \rightarrow 0_1^+$. A strong self coincidence is visible at this energy range, much stronger than in the case of ^{84}Ge, which is a hint for the 510(19)/534(8)-keV doublet in this energy range. Furthermore, the transition at

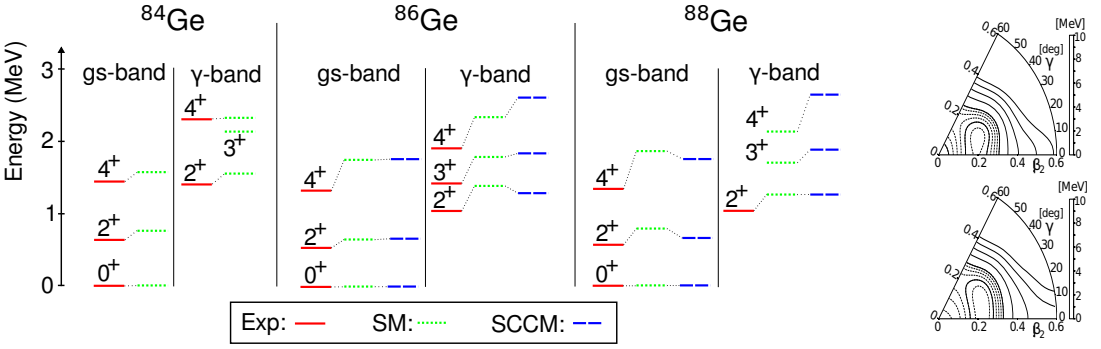

Figure 3. (left) Systematics of the ^{84,86,88}Ge level energies from experiment compared to theoretical predictions from shell model (SM) and SCCM. The shell model calculation for ^{84}Ge is taken from [29] (right) Potential energy surfaces in the particle number variation after projection (PN-VAP) approach [30] for ^{86}Ge (top) and ^{88}Ge (bottom). The spacing between solid contour lines is 2 MeV with intermediate dashed lines for 0.5 MeV steps. The minima are located at about $\beta_2 = 0.2$.

1057(22) keV is absent in the $\gamma\gamma$ coincidence. Therefore, the 1057(22)-keV-γ ray is assigned to the $(2_2^+) \rightarrow (0_1^+)$ transition and the doublet to the competitive $(2_2^+) \rightarrow (2_1^+) \rightarrow (0_1^+)$ decay path. Based on comparison to ^{84}Ge, the transitions at 865(18) keV and 1180(26) keV are assigned to the $(4_2^+) \rightarrow (2_2^+)$ and $(6_1^+) \rightarrow (4_1^+)$ decays, respectively. The transition at 380(8) keV is visible in the $\gamma\gamma$ coincidence gate of the $(2_1^+)/(2_2^+)$ doublet and appears in a gate on the $(2_2^+) \rightarrow (0_1^+)$ transition shown in figure 1 (e) as well. Gating in the neighboring region of $\sim$ 1360 keV the 380(8)-keV transition is absent. This transition is assigned to originate from the $(3_1^+) \rightarrow (2_2^+)$ decay (for details, see [1]).
The Doppler-corrected γ-ray spectrum of ^{88}Ge after a ^{89}As(p,2p) reaction is shown in figure 1 (f). It is the first spectroscopy of ^{88}Ge, thus the three transitions at energies of 469(14) keV, 556(6) keV and 772(33) keV are observed for the first time. The suggested level scheme for ^{88}Ge is shown in figure 2 on the right. According to the assignments before, the strongest transition in the spectrum is assigned to be the $2_1^+ \rightarrow 0_1^+$ transition. A $\gamma\gamma$ coincidence gate on its energy range is shown in figure 1 (g), yielding both transitions. In comparison to ^{86}Ge the γ-ray at 772(33) keV is assigned to the $(4_1^+) \rightarrow (2_1^+)$ transition, and the γ-ray at 469(14) keV is assigned to the $(2_2^+) \rightarrow (2_1^+)$ transition.

4. Discussion

In the following, the obtained results are compared to a shell-model calculation and to a symmetry-conserving configuration mixing Gogny (SCCM) calculation. The left side of figure 3 shows the comparison of the constructed level schemes and the predictions from both theories. Both theoretical predictions of the level sequences are in good agreement with the experiment, whereas the theories overestimate the level energies systematically. The low-lying γ band predicted from both theories, which is pointing to triaxial features of the isotopes, is reproduced by the measured data. Furthermore, both theories predict a 3_1^+ state in ^{86}Ge which is closer to the 2_2^+ state than to the 4_2^+ state, in contrast to ^{84}Ge and ^{88}Ge, where it is predicted to be closer to the 4_2^+ state than to the 2_2^+ state or rater central. A promising candidate for this state is observed through the 380(8)-keV transition in this experiment. This state at 1426(16) keV would dominantly decay to the 2_2^+ state with such a 380(8)-keV transition. With this assignment an $S(4) = 0.20(4)$ staggering parameter is obtained for ^{86}Ge, even larger than for ^{76}Ge where a staggering of $S(4) = 0.091(2)$ [7] has been observed. This reflects an even

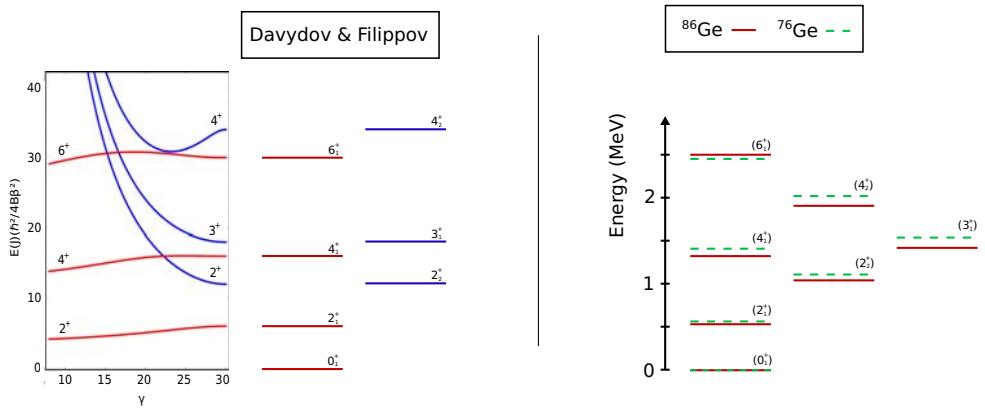

Figure 4. (left) Evolution of the ground-state band and γ-band energies with increasing deformation parameter γ calculated with the model of Davydov and Filippov [4]. (middle) Low-energy level scheme calculated by the model of Davydov and Filippov for $\gamma = 30°$. (right) Comparison of the low-spin spectra of ^{76}Ge and ^{86}Ge.

larger degree of triaxiality in ^{86}Ge than in ^{76}Ge. The similarities of ^{76}Ge and ^{86}Ge are shown in figure 4 in the right. The states in the ground-state and γ band match within 100 keV in both nuclei. In addition, figure 4 (left) shows the behavior of the ground-state band and the γ-band for an increasing deformation parameter γ calculated by the model of Davydov and Filippov. The resulting spectrum for $\gamma = 30°$ is shown in the center of the figure. Besides the distinct reproduction of the ground-state band, the position of the γ-band head is in good agreement with experiment. From the evolution of the 2_2^+ level energy with increasing γ it can be seen that its energy drops below the 4_1^+ level energy for $\gamma > 22°$. Within the model of Davydov and Filippov the γ of ^{86}Ge can be calculated by [31]

$$\frac{E_{2_2^+}}{E_{2_1^+}} = \frac{1 + \sqrt{1 - \frac{8}{9}\sin^2 3\gamma}}{1 - \sqrt{1 - \frac{8}{9}\sin^2 3\gamma}}. \tag{2}$$

From data we obtain $E_{2_2^+}/E_{2_1^+} = 1.98(3)$. This yields $\gamma = 30(1)°$, as expected for a pronounced triaxial shape. The observation of rigid triaxiality is further extended by the energy surfaces from the SCCM calculation shown in figure 3. A pronounced triaxial minimum is predicted for ^{86}Ge, while more γ softness is predicted for ^{88}Ge.

5. Summary

For the first time, γ-ray spectroscopy of ^{88}Ge has been performed. By means of in-flight γ-ray spectroscopy of ^{84,86,88}Ge 16 transitions have been studied, 10 of which have been observed for the first time. Based on informations of neighboring Ge isotopes and the knowledge from former $(p, 2p)$ studies in this region of the nuclear chart new level schemes for ^{86}Ge and ^{88}Ge are proposed. For ^{86}Ge a candidate for a 3_1^+ state was observed. With this assignment a staggering parameter $S(4) = 0.20(4)$ was obtained for ^{86}Ge, which is even bigger than for the so far known case of ^{76}Ge. Interpreted with the model from Davydov and Filippov, ^{86}Ge is assigned as an example for a pronounced triaxial shape of a nucleus. This is in good agreement with state-of-the-art theoretical predictions in this region.

Acknowledgements
The authors thank the RIBF and BigRIPS teams for providing a stable, high-intensity uranium beam and operating the secondary beams. We acknowledge support from the German BMBF Grant Nos. 05P12RDFN1, 05P12RDFN8 and 05P15PKFNA, the ERC Grant No. MINOS-258567, the Spanish Ministerio de Economía y Competitividad under contracts FPA2014-57196-C5-4-P and FIS−2014−53434, the Vietnam Ministry of Science and Technology, as well as from the Science and Technology Facilities Council (STFC). We further thank GSI for providing computing facilities.

References

[1] M. Lettmann *et al.*, Phys. Rev. C **96**, 011301(R) (2017)
[2] A. Bohr and B. Mottelson, Mat. Fys. Medd. Dan. Vid. Selsk. **27** (1958)
[3] L. Wilets and M. Jean, Phys. Rev. **102**, 788 (1956)
[4] A. S. Davydov and G. F. Filippov, Nucl. Phys. **8**, 237 (1958)
[5] N. V. Zamfir and R. F. Casten, Phys. Lett. B **260**, 265 (1991)
[6] E. A. McCutchan, D. Bonatsos, N. V. Zamfir, R. F. Casten, Phys. Rev. C **76** 024306(R) (2007)
[7] Y. Toh *et al.*, Phys. Rev. C **87** 041304(R) (2013)
[8] T. Kubo *et al.*, Prog. Theor. Exp. Phys. **2012** 03C003 (2012)
[9] N. Fukuda, *et al.*, Nucl. Instrum. Methods Phys. Res. B **317** 323-332 (2013)
[10] A. Obertelli, *et al.*, Eur. Phys. J. A **50** 8 (2014)
[11] C. Santamaria, *et al.*, in preparation (2017)
[12] S. Takeuchi, *et al.*, Nucl. Instrum. Methods Phys. Res. A **763** 8 (2014)
[13] P. Doornenbal, Prog. Theor. Exp. Phys. **2012** 03C004 (2012)
[14] C. Santamaria, *et al.*, Phys. Rev. Lett. **115** 192501 (2015)
[15] S. Chen, *et al.*, Phys. Rev. C **95** 041302(R) (2017)
[16] F. Flavigny, *et al.*, Phys. Rev. Lett. **118** 242501 (2017)
[17] N. Paul, *et al.*, Phys. Rev. Lett. **118** 032501 (2017)
[18] C. M. Shand, *et al.*, Phys. Lett. B **773** 492-497 (2017)
[19] L. Olivier, *et al.*, Phys. Rev. Lett., accepted (2017)
[20] S. Agostinelli, *et al.*, Nucl. Instrum. Methods Phys. Res. A **506** 250-303 (2003)
[21] A. Korgul *et al.*, Phys. Rev. C **88** 044330 (2013)
[22] K. Kolos *et al.*, Phys. Rev. C **88** 047301 (2013)
[23] J. A. Winger *et al.*, Phys. Rev. C **81** 044303 (2010)
[24] K. Miernik *et al.*, Phys. Rev. Lett. **111** 132502 (2013)
[25] P. Doornenbal *et al.*, Phys. Rev. Lett. **111** 212502 (2013)
[26] H. Iwasaki *et al.*, Phys. Rev. Lett. **112** 142502 (2014)
[27] D. Bazin *et al.*, Phys. Rev. Lett. **91** 012501 (2003)
[28] P. Fallon *et al.*, Phys. Rev. C. **81** 041302 (2010)
[29] K. Sieja, T. R. Rodríguez, K. Kolos, D. Verney, Phys. Rev. C. **88** 034327(R) (2013)
[30] M. Anguiano, J. L. Egido, L. M. Robledo, Phys. Lett. B **545** 62-72 (2002)
[31] A. S. Davydov and V. S. Rostovsky, Nucl. Phys. **12** 58-68 (1959)